Spectrochimica Acta Part A: Molecular and Biomolecular Spectroscopy 118 (2014) 430–437

Contents lists available at ScienceDirect

Spectrochimica Acta Part A: Molecular and Biomolecular Spectroscopy

journal homepage: www.elsevier.com/locate/saa

Raman, infrared and near-infrared spectroscopic characterization of the herderite–hydroxylherderite mineral series

Ray L. Frost [a,*], Ricardo Scholz [b], Andrés López [a], Yunfei Xi [a], Camila de Siqueira Queiroz [b], Fernanda M. Belotti [c], Mauro Cândido Filho [d]

[a] School of Chemistry, Physics and Mechanical Engineering, Science and Engineering Faculty, Queensland University of Technology, GPO Box 2434, Brisbane, Queensland 4001, Australia
[b] Geology Department, School of Mines, Federal University of Ouro Preto, Campus Morro do Cruzeiro, Ouro Preto, MG 35400-00, Brazil
[c] Federal University of Itajubá, Campus Itabira, Itabira, MG, Brazil
[d] Mining Engineering Department, School of Mines, Federal University of Ouro Preto, Campus Morro do Cruzeiro, Ouro Preto, MG 35400-00, Brazil

HIGHLIGHTS

- We have studied herderite–hydroxylherderite series from Brazil.
- $CaBePO_4(F,OH)$ was investigated by an electron microprobe.
- The minerals occur as secondary products in granitic pegmatites.
- We studied the minerals using vibrational spectroscopy.
- Hydrogen bond distances were calculated.

GRAPHICAL ABSTRACT

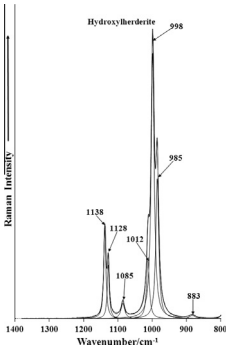

ARTICLE INFO

Article history:
Received 10 June 2013
Received in revised form 27 August 2013
Accepted 2 September 2013
Available online 13 September 2013

Keywords:
Raman spectroscopy
Herderite
Hydroxylherderite
Phosphate
Beryllium
Pegmatite

ABSTRACT

Natural single-crystal specimens of the herderite–hydroxylherderite series from Brazil, with general formula $CaBePO_4(F,OH)$, were investigated by electron microprobe, Raman, infrared and near-infrared spectroscopies. The minerals occur as secondary products in granitic pegmatites. Herderite and hydroxylherderite minerals show extensive solid solution formation. The Raman spectra of hydroxylherderite are characterized by bands at around 985 and 998 cm^{-1}, assigned to v_1 symmetric stretching mode of the $HOPO_3^{3-}$ and PO_4^{3-} units. Raman bands at around 1085, 1128 and 1138 cm^{-1} are attributed to both the HOP and PO antisymmetric stretching vibrations. The set of Raman bands observed at 563, 568, 577, 598, 616 and 633 cm^{-1} are assigned to the v_4 out of plane bending modes of the PO_4 and H_2PO_4 units. The OH Raman stretching vibrations of hydroxylherderite were observed ranging from 3626 cm^{-1} to 3609 cm^{-1}. The infrared stretching vibrations of hydroxylherderites were observed between 3606 cm^{-1} and 3599 cm^{-1}. By using a Libowitzky type function, hydrogen bond distances based upon the OH stretching bands were calculated. Characteristic NIR bands at around 6961 and 7054 cm^{-1} were assigned to the first overtone of the fundamental, whilst NIR bands at 10,194 and 10,329 cm^{-1} are assigned to the second overtone of the fundamental OH stretching vibration. Insight into the structure of the herderite–hydroxylherderite series is assessed by vibrational spectroscopy.

Introduction

Beryllium is a typical chemical element found in granitic pegmatites, especially in the structure of silicates such as beryl [$Be_3Al_2(Si_6O_{18})$], phenakite (Be_2SiO_4), euclase [$(BeAl(SiO_4)(OH)$]

* Corresponding author. Tel.: +61 7 3138 2407; fax: +61 7 3138 1804.
E-mail address: r.frost@qut.edu.au (R.L. Frost).

1386-1425/$ - see front matter © 2013 Elsevier B.V. All rights reserved.
http://dx.doi.org/10.1016/j.saa.2013.09.021

and bertrandite [$Be_4(Si_2O_7)(OH)_2$], and the oxide chrysoberyl ($BeAl_2O_4$). Beryllium metal is an important element in industry with different applications in metallurgy especially in the production of copper, aluminum and magnesium alloys; however, the use is limited due to the high price and toxicity. Beryllium has also importance for the defence and aerospace industry, due to its stiffness, light weight and dimensional stability over a wide temperature range. Despite the importance for industry, the major field of use of beryllium minerals is in the gemstones and jewelry market, mainly, emerald and aquamarine [1].

Be phosphates are relatively rare in nature and are related to a range of temperature and pressure during the pegmatite evolution [2], occurring from the magmatic process [3,4] to the hydrothermal and supergene [5,6]. Černý [7] and Černá et al. [8] describes beryllium phosphates as secondary product of late alteration of beryl. The most common Be phosphates are hydroxylherderite, moraesite, beryllonite and the members of the roscherite group [7–10]. Herderite and hydroxylherderite are two rare gemstones and also shows importance in the mineral collectors market [11–13]. Herderite was first described from samples associated with the Sn-bearing pegmatites at Ehrenfriedersdorf in the Erzgebirge of Germany [14], and hydroxylherderite was first described from the mineral District of Paris, Maine, USA by Penfield [15] as hydro-herderite. Later, Palache et al. [16] were responsible to establish the herderite–hydroxylherderite series. Byrappa and Pushcharovsky [17] have observed the structural similarity between hydroxylherderite and datolite. Chrystallographic studies were carried out by Lager and Gibbs [18] in hydroxylherderite from Golconda pegmatite, in Brazil and Harlow and Hawthorn [19] have solved the crystal structure of herderite from Mogok, Myanmar.

According to Lager and Gibbs [18], hydroxylherderite crystallizes in the monoclinic system, $P2_1/a$ space group, with $a = 9.789(2)$ Å, $b = 7.661(1)$ Å, $c = 4.804(1)$ Å and $\beta = 90.02(1)°$. Hydroxylherderite consists of sheets of corner-sharing PO_4 and BeO_3OH tetrahedra linked along the c axis by sheets of edge-sharing Ca-containing polyhedral. Each tetrahedral sheet contains alternating PO_4 and BeO_3OH polyhedral which form a network of four- and eight-membered centro-symetric rings extending parallel to (0 0 1). Herderite, as described by Harlow and Hawthorn [19] crystallizes in monoclinic crystal system, space group $P2_1/a$, with $a = 9.7446(4)$ Å, $b = 7.6769(3)$ Å, $c = 4.7633(2)$ Å, $\beta = 90.667(1)°$, $V = 356.31(4)$ Å^3, and $Z = 4$. The authors cited that as effect of increasing of herderite content, generally occurs a contraction of the structure, with a decrease in a, c, and V and the increase in b. The relation F—OH in herderite and hydroxylherderite were also studied in different ways. In a systematic optical and chemical characterization, Leavens et al. [20] have described the dependence of the refractive index with the F/OH ratios and have established the increase of refractive index to the decrease of F content.

In the infrared spectroscopic characterization of the amblygonite–montebrasite mineral series, Fransolet and Tarte [21] established a correlation between OH wavenumbers (ν_{OH} in the region between 3400–3350 cm^{-1} and δ_{OH} in the 840–800 cm^{-1} region) and the fluorine content. With the application of Raman spectroscopy, Rondeau et al. [22] have observed correlation between the F content with the position of 3 characteristic Raman peaks and the full width at medium height (FWMH) of the peak around 3370 cm^{-1}.

Farmer [23] divided the vibrational spectra of phosphates according to the presence, or absence of water and hydroxyl units in the minerals. In aqueous systems, Raman spectra of phosphate oxyanions show a symmetric stretching mode (ν_1) at 938 cm^{-1}, the antisymmetric stretching mode (ν_3) at 1017 cm^{-1}, the symmetric bending mode (ν_2) at 420 cm^{-1} and the ν_4 mode at 567 cm^{-1} [24–28]. The value for the ν_1 symmetric stretching vibration of PO_4 units as determined by infrared spectroscopy was given as 930 cm^{-1} (augelite), 940 cm^{-1} (wavellite), 970 cm^{-1} (rockbridgeite), 995 cm^{-1} (dufrenite) and 965 cm^{-1} (beraunite). The position of the symmetric stretching vibration is mineral dependent and a function of the cation and crystal structure. The fact that the symmetric stretching mode is observed in the infrared spectrum affirms a reduction in symmetry of the PO_4 units.

The value for the ν_2 symmetric bending vibration of PO_4 units as determined by infrared spectroscopy was given as 438 cm^{-1} (augelite), 452 cm^{-1} (wavellite), 440 and 415 cm^{-1} (rockbridgeite), 455, 435 and 415 cm^{-1} (dufrenite) and 470 and 450 cm^{-1} (beraunite). The observation of multiple bending modes provides an indication of symmetry reduction of the PO_4 units. This symmetry reduction is also observed through the ν_3 antisymmetric stretching vibrations. Augelite [28]shows infrared bands at 1205, 1155, 1079 and 1015 cm^{-1}; wavellite at 1145, 1102, 1062 and 1025 cm^{-1}; rockbridgeite at 1145, 1060 and 1030 cm^{-1}; dufrenite at 1135, 1070 and 1032 cm^{-1}; and beraunite at 1150, 1100, 1076 and 1035 cm^{-1}.

Published data concerning the spectroscopic characterization of beryllium phosphates are very rare in the literature. In the characterization of fluid inclusions in quartz from granitic pegmatites, Rickers et al. [29] describes Raman bands in herderite at 584, 595, 983, 1005 cm^{-1}; however, the authors gave no assignment of the bands. In recent studies, in reference to the datas published by Rickers et al. [29], Frezzoti et al. [30] described Raman vibrations related to $(PO_4)^{3-}$ anion in herderite at 584 cm^{-1} (ν_4), 983 cm^{-1} (ν_1) and 1005 (ν_3) cm^{-1}.

The objectives of this work are to understand the structure of herderite–hydroxylherderite minerals with the application of the vibrational spectroscopic methods infrared and Raman spectroscopy and to establish a relation between the F/OH ratios and the position of the vibrations bands of OH^- anion.

Experimental

Occurrence, sample description and preparation

For the development of this work, three natural single crystal specimens of the hydroxylherderite series were chosen. The samples were collected from different pegmatites and incorporated into the collection of the Geology Department of the Federal University of Ouro Preto, Minas Gerais, Brazil.

Sample SAA-073 was collected from the Morro Redondo mine, which belongs to the Araçuai pegmatite district, located near Coronel Murta, north of Minas Gerais. It corresponds to a bluish 3.0 cm single crystal and was found in association with muscovite and albite in a miarolitic cavity. Sample SAA-074 was collected from Jove Lauriano mine, located in the Conselheiro Pena pegmatite district, municipality of Divino das Laranjeiras, east of Minas Gerais. It corresponds to a single crystal up to 2 cm with yellowish color. The crystal was found in association with muscovite and albite in a miarolitic cavity. Samples SAA-075 and SAA-076 were also collected from pegmatites in the municipality of Divino das Laranjeiras. SAA-075 corresponds to an aggregate of 0.4 cm colorless single crystals and was found in association with muscovite, albite and fluorapatite in a miarolitic cavity. SAA-076 was collected from the Almerindo mine [31]. It corresponds to a yellowish single crystal, up to 2 cm in length and was found in association with muscovite, albite, fluorapatite and brazilianite in a miarolitic cavity. Sample SAA-093 was collected from a muscovite and topaz pegmatite in Medina, north from Minas Gerais. The single crystal shows bluish color, and occurs in association with muscovite.

The calcium and beryllium phosphates herderite and hydroxylherderite are the end member of a solid solution between fluorine and hydroxyl anions. The minerals occur in miarolitic

cavities of granitic pegmatites, in different mineral associations. The samples were collected from five different Brazilian pegmatites. Four samples are related to lithium bearing pegmatites: SAA-073 (Morro Redondo – lepidolite and elbaite), SAA-074 (Jove Lauriano – montebrasite type and minor spodumene), SAA-075 (Osvaldo Perini – montebrasite type), SAA-076 (Almerindo – triphylite type) and one sample was collected from a muscovite-topaz rich pegmatite (Medina – SAA-093). Samples SAA-073, SAA-074 and SAA-075 are labeled as a, b, c in the figures.

The crystals were hand selected and phase analyzed by X-ray powder diffraction for simple identification. Fragments of each sample were prepared in different ways to be submitted to chemical analysis by Electron microprobe, Raman and infrared spectroscopy.

Electron microprobe analysis (EMP)

Chemical characterization was carried via EMP. Each sample selected for this study was analyzed with the performance of five spots per crystal. The chemical analysis was carried out with a Jeol JXA8900R spectrometer from the Physics Department of the Federal University of Minas Gerais, Belo Horizonte. For each selected element was used the following standards: Ca–Apatite, P—$Ca_2P_2O_7$, F–Fluorite, Mn–Rhodonite, Fe–Magnetite, Al—Al_2O_3 and Mg—MgO. Be and H_2O were calculated by stoichiometry. The epoxy embedded hydroxylherderite samples were coated with a thin layer of evaporated carbon. The electron probe microanalysis in the WDS (wavelength dispersive spectrometer) mode was obtained at 15 kV accelerating voltage and beam current of 10 nA. Chemical formula was calculated on the basis of five oxygen atoms (O, F, OH).

Raman microprobe spectroscopy

Crystals of herderite/hydroxylherderite were placed on a polished metal surface on the stage of an Olympus BHSM microscope, which is equipped with 10×, 20×, and 50× objectives. The microscope is part of a Renishaw 1000 Raman microscope system, which also includes a monochromator, a filter system and a CCD detector (1024 pixels). The Raman spectra were excited by a Spectra-Physics model 127 He—Ne laser producing highly polarized light at 633 nm and collected at a nominal resolution of 2 cm^{-1} and a precision of ±1 cm^{-1} in the range between 200 and 4000 cm^{-1}. Repeated acquisitions on the crystals using the highest magnification (50×) were accumulated to improve the signal to noise ratio of the spectra. The spectra were collected over night. Raman Spectra were calibrated using the 520.5 cm^{-1} line of a silicon wafer. The Raman spectrum of at least 10 crystals was collected to ensure the consistency of the spectra.

Infrared spectroscopy

Infrared spectra were obtained using a Nicolet Nexus 870 FTIR spectrometer with a smart endurance single bounce diamond ATR cell. Spectra over the 4000–525 cm^{-1} range were obtained by the co-addition of 128 scans with a resolution of 4 cm^{-1} and a mirror velocity of 0.6329 cm/s. Spectra were co-added to improve the signal to noise ratio.

Near-infrared spectroscopy

NIR spectra were collected on a Nicolet Nexus FT-IR spectrometer with a Nicolet Near-IR Fibreport accessory (Madison, Wisconsin). The reason for using a fibre optic probe is the ease of operation and the fact that the probe can be brought to the mineral and can be used at some distance from the spectrometer. A white light source was used, with a quartz beam splitter and TEC NIR InGaAs detector. Spectra were obtained from 13,000 to 4000 cm^{-1} (0.77–2.50 μm) by the co-addition of 256 scans at a spectral resolution of 8 cm^{-1}. A mirror velocity of 1.266 m s^{-1} was used. The spectra were transformed using the Kubelka–Munk algorithm to provide spectra for comparison with published absorption spectra.

Spectral manipulation such as baseline correction/adjustment and smoothing were performed using the Spectracalc software package GRAMS (Galactic Industries Corporation, NH, USA). Band component analysis was undertaken using the Jandel 'Peakfit' software package that enabled the type of fitting function to be selected and allows specific parameters to be fixed or varied accordingly. Band fitting was done using a Lorentzian–Gaussian cross-product function with the minimum number of component bands used for the fitting process. The Lorentzian–Gaussian ratio was maintained at values greater than 0.7 and fitting was undertaken until reproducible results were obtained with squared correlations of r^2 greater than 0.995.

Results and discussion

Chemical characterization

The chemical composition of hydroxylherderite–herderite samples are presented in Table 1. For all analyzed samples the phosphorous content was slightly higher and Ca content slightly lower than expected for ideal herderite/hydroxylherderite composition (ideal herderite: [P_2O_5] 43.53 wt.%; [CaO] 34.39 wt.%; hydroxylherderite: [P_2O_5] 44.06 wt.%; [CaO] 34.82 wt.%). Low iron and manganese impurity contents were found in all four samples, and calcium impurities were found in samples SAA-073 and SAA-074.

Total formula calculations were performed considering BeO and H_2O content calculated by stoichiometry for all samples. The H_2O concentration in wt.% was calculated for the ideal formula of $CaBePO_4(F_xOH_{1-x})$ using the fluorine concentration measured by EMP. The results indicate clearly that samples SAA-073, SAA-074 and SAA-075 belong to hydroxylherderite with high OH content. Only sample SAA-076 shows lower OH content, belongs to an intermediate member in the herderite–hydroxylherderite series.

Vibrational spectroscopy background

In aqueous systems, the Raman spectra of phosphate oxyanions show a symmetric stretching mode (ν_1) at 938 cm^{-1}, an antisymmetric stretching mode (ν_3) at 1017 cm^{-1}, a symmetric bending mode (ν_2) at 420 cm^{-1} and a ν_4 bending mode at 567 cm^{-1} [25,27,32]. S.D. Ross in Farmer listed some well-known minerals containing phosphate which were either hydrated or hydroxylated or both [23]. The vibrational spectrum of the dihydrogen phosphate anion has been reported by Farmer [23]. The PO_2 symmetric stretching mode occurs at 1072 cm^{-1} and the POH symmetric stretching mode at ~878 cm^{-1}. The POH antisymmetric stretching mode was found at 947 cm^{-1} and the $P(OH)_2$ bending mode at 380 cm^{-1}. The band at 1150 cm^{-1} was assigned to the PO_2 antisymmetric stretching mode. The position of these bands will shift according to the crystal structure of the mineral.

The vibrational spectra of phosphate minerals have been published by Farmer's treatise Chapter 17 [23]. The Table 17.III in Ref. [23] reports the band positions of a wide range of phosphates and arsenates. The band positions for the monohydrogen phosphate anion of disodium hydrogen phosphate dihydrate is given as ν_1 at 820 and 866 cm^{-1}, ν_2 at around 460 cm^{-1}, ν_3 as 953, 993, 1055, 1070, 1120 and 1135 cm^{-1}, ν_4 at 520, 539, 558,

Table 1
Electron microprobe analysis of hydroxylherderite-herderite samples in wt.%. The result was taken as the mean value from five spots. H_2O and BeO were calculated by stoichiometry.

Sample	P_2O_5		MnO		FeO		CaO		Al_2O_3		BeO	F		H_2O	O=F	Total
SAA-073	41.86	40.94–42.73	0.15	0.00–0.65	0.01	0.00–0.02	33.29	32.65–33.79	0.02	0.00–0.05	15.52	0.24	0.09–0.37	5.28	−0.10	96.28
SAA-074	42.57	41.95–43.03	0.01	0.00–0.03	0.01	0.00–0.04	33.89	33.61–34.30	0.02	0.00–0.06	15.52	0.07	0.00–0.15	5.42	−0.03	97.50
SAA-075	42.46	41.56–43.55	0.07	0.03–0.13	0.01	0.00–0.06	33.73	33.45–33.93	0.02	0.00–0.03	15.48	1.90	1.75–2.05	4.53	−0.80	97.42
SAA-076	42.85	42.42–43.68	0.02	0.00–0.03	0.01	0.00–0.04	34.19	33.71–34.46	0.02	0.00–0.06	15.43	4.46	4.19–4.59	3.37	−1.88	98.49
SAA-093	42.23	41.76–43.11	0.03	0.00–0.07	0.01	0.00–0.05	32.59	32.14–32.92	0.01	0.00–0.03	15.43	8.01	7.73–8.20	1.58	−3.39	96.56
20,517[b]	43.98	–	ND	–	0.01	–	34.99	–	0.01	–	15.54	5.71	–	2.90	−2.40	100.76
Herderite[a]	43.53		0.00		0.00		34.39		0.00		15.34	11.65		0.00		100.00
Hydroxylherderite[a]	44.06		0.00		0.00		34.82		0.00		15.53	0.00		5.59		100.00
	P		Mn		Fe		Ca		Al		Be	F		OH		
SAA-073	0.99		0.00		0.00		0.99		0.00		1	0.02		0.98		3.98
SAA-074	0.99		0.00		0.00		1.00		0.00		1	0.01		0.99		3.99
SAA-075	0.99		0.00		0.00		1.00		0.00		1	0.17		0.83		3.99
SAA-076	0.99		0.00		0.00		1.00		0.00		1	0.39		0.61		3.99
SAA-093	1.00		0.00		0.00		0.97		0.00		1	0.71		0.29		3.97
20,517[b]	0.997		–		0.000		1.004		0.000		1	0.483		0.517		3.994
Herderite[a]	1.0		0.00		0.00		1.0		0.00		1.0	1.0		0.0		4.0
Hydroxylherderite[a]	1.0		0.00		0.00		1.0		0.00		1.0	0.0		1.0		4.0

[a] Calculated on the basis of ideal formula of herderite–($CaBe(PO_4)(F)$ and hydroxylherderite–($CaBe(PO_4)(OH)$.
[b] According to Harlow and Hawthorne [19].

575 cm^{-1}. The POH unit has vibrations associated with the OH specie. The stretching vibration of the POH units was tabulated as 2430 and 2870 cm^{-1}, and bending modes at 766 and 1256 cm^{-1}. Water stretching vibrations were found at 3050 and 3350 cm^{-1}. The position of the bands for the disodium hydrogen phosphate is very dependent on the waters of hydration. There have been several Raman spectroscopic studies of the monosodium dihydrogen phosphate chemicals [33–37].

Raman and infrared spectroscopy

The Raman spectrum of hydroxylherderite is illustrated in Fig. 1. Clearly there are large parts of the spectrum where no intensity is observed. Therefore, the spectra are subdivided into sections according to the types of molecular vibrations being observed. The infrared spectrum of hydroxylherderite is shown in Fig. 2. As with the Raman spectrum, no intensity is observed in large parts of the spectrum and as a consequence, the spectrum may be subdivided into sections according to the types of vibrations being observed. The Raman spectra of the three samples shown (samples SAA073, SAA075 and SAA076) in this spectral region are very similar, although some variation in band position is observed.

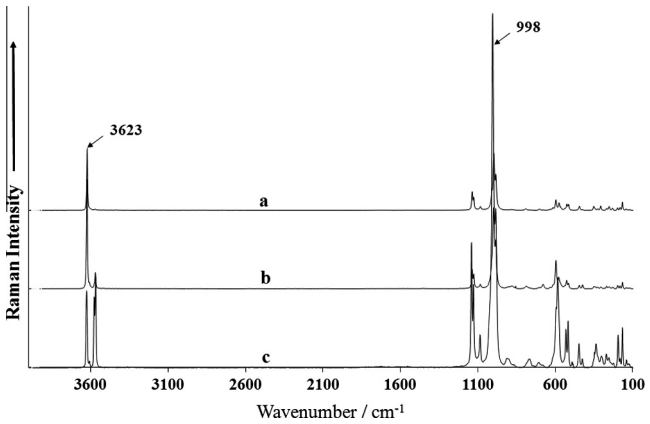

Fig. 1. Raman spectra of hydroxylherderite in the 100–4000 cm^{-1} region.

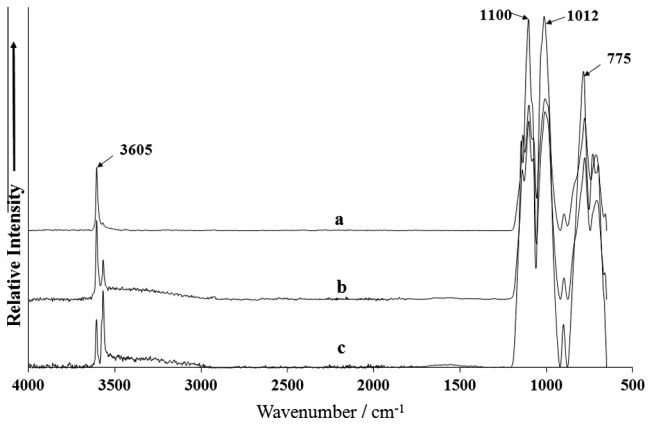

Fig. 2. Infrared spectra of hydroxylherderite in the 500–4000 cm^{-1} region.

The Raman band at 998 cm^{-1} of hydroxylherderite is assigned to the ν_1 symmetric stretching mode of the PO_4^{3-} units. The band is observed at 1000 cm^{-1} for sample b and 1006 cm^{-1} for sample c. The Raman spectrum of herderite displays a band at 975 cm^{-1}. Raman spectra of herderite were found very difficult to obtain because of fluorescence. The band at 985 cm^{-1} for hydroxylherderite is attributed to the $HOPO_3^{3-}$ units. Galy [35] first studied the polarized Raman spectra of the $H_2PO_4^-$ anion. Choi et al. reported the polarization spectra of NaH_2PO_4 crystals. Casciani and Condrate [38] published spectra on brushite and monetite together with synthetic anhydrous monocalcium phosphate ($Ca(H_2PO_4)_2$), monocalcium dihydrogen phosphate hydrate ($Ca(H_2PO_4)_2{\cdot}H_2O$) and octacalcium phosphate ($Ca_8H_2(PO_4)_6{\cdot}5H_2O$). These authors determined band assignments for $Ca(H_2PO_4)$ and reported bands at 1012 and 1085 cm^{-1} as POH and PO stretching vibrations, respectively. The two Raman bands at 1128 and 1138 cm^{-1} are attributed to both the HOP and PO antisymmetric stretching

vibrations. Casciani and Condrate [38] tabulated Raman bands at 1132 and 1155 cm^{-1} and assigned these bands to P—O symmetric and the P—O antisymmetric stretching vibrations. It is proposed that the proton on the hydroxyl units is very liable and can oscillate between the OH units and the phosphate units. In this way the hydrogen phosphate units are formed. Raman bands in the 883–908 cm^{-1} are assigned to hydroxyl deformation modes. The position and number of bands in this part of the spectrum is a function of the degree of fluorine substitution. In sample a, it is suggested that the amount of hydroxyl units is low, when compared with samples b and c where distinct OH deformation modes are observed.

The infrared spectrum of hydroxylherderite (Fig. 2) shows very intense bands at 1012 cm^{-1} assigned to the ν_1 symmetric stretching mode of the PO_4^{3-} units. The infrared spectrum of herderite shows an intense band at 1005 cm^{-1} and is attributed to this vibration. The infrared bands at around 1100 cm^{-1} are assigned to the ν_3 antisymmetric stretching mode of the PO_4^{3-} units. The infrared bands of herderite at 1079, 1099, 1121 and 1149 cm^{-1} are assigned to this vibrational mode.

Some variation in peak position and intensity is observed in the Raman spectra of the three hydroxylherderite samples. The set of Raman bands of hydroxylherderite observed at 563, 568, 577, 598, 616 and 633 cm^{-1} (sample a), 568, 579, 597, 616 and 534 cm^{-1} and 578, 586, 597 and 614 cm^{-1} (sample c) are assigned to the ν_4 out of plane bending modes of the PO_4 and H_2PO_4 units. The Raman bands in this part of the spectral region for herderite were swamped by fluorescence. The Raman spectrum of NaH_2PO_4 shows Raman bands at 526, 546 and 618 cm^{-1}. The observation of multiple bands in this spectral region supports the concept of symmetry reduction of both the phosphate and hydrogen phosphate units. The Raman bands at 425 and 446 cm^{-1} together with the bands at 516 and 527 cm^{-1} (sample a), 426, 447, 516 and 528 cm^{-1} (sample b) and 427, 449, 493, 529 and 533 cm^{-1} (sample c) are attributed to the ν_2 PO_4 and H_2PO_4 bending modes. The Raman spectrum of NaH_2PO_4 shows two Raman bands at 460 and 482 cm^{-1}. The observation of multiple Raman bands for the hydroxylherderite mineral supports the concept of symmetry reduction.

A number of bands are observed in the 300–350 cm^{-1} region. Raman bands are found at 308, 327, 346 and 354 cm^{-1} (sample a), 307, 328, 343 and 352 cm^{-1} (sample b) and 303, 325, 339, 349 and 355 cm^{-1} are attributed to BeO and CaO stretching vibrations. Some varaition in band position and intensity is observed. This is expected as these bands are due to external or often called lattice vibrations. Strong Raman bands are found at 145, 168, 184, 199, 232, 254 and 270 cm^{-1} (sample a), 168, 184, 198, 230, 254 and 170 cm^{-1} (sample b), 168, 183, 196, 254 and 272 cm^{-1} (sample c).

The Raman spectrum of the OH stretching region may be observed in Fig. 1.

This spectral region is where the OH stretching vibrations are observed. In this spectral region, considerable variation in intensity is observed. For sample a, a single intense Raman band at 3623 cm^{-1} is observed with a low intensity shoulder at 3622 cm^{-1}. Another low intensity band is observed at 3570 cm^{-1}. This latter band shows greater intensity for sample b. For this sample a very intense band at 3624 cm^{-1} is found, now with a low intensity shoulder at 3627 cm^{-1}. A low intensity band at 3609 cm^{-1} is also found. The band at 3570 cm^{-1} for hydroxylherderite samples a and b now is split into two bands at 3568 and 3578 cm^{-1} for sample c and shows much greater intensity. The Raman spectrum of herderite displays an intense sharp band at 3625 cm^{-1} with a low intensity shoulder on the low wavenumber side of the main peak. It is significant that there are two OH stretching vibrations; thus, indicating that there are two non-equivalent OH units.

The infrared spectrum of sample a shows a very intense band at 3605 cm^{-1} with low wavenumber shoulders at 3569 and 3597 cm^{-1} (Fig. 2). The infrared spectrum is in good harmony with the Raman spectrum of this sample. The infrared spectrum for sample b displays an intense band at 3605 cm^{-1} with shoulders at 3570 and 3599 cm^{-1}. These bands are attributed to the OH stretching vibration. Two peaks of around equal intensity for herderite are observed at 3567 and 3575 cm^{-1}. The observation of multiple bands supports the concept that the OH units are not equivalent. The OH peaks are superimposed upon a broad feature centered around 3640 cm^{-1} and attributed to adsorbed water. For sample c, two intense infrared peaks are observed at 3566 and 3605 cm^{-1} with a shoulder band at 3600 cm^{-1}. Again, the OH stretching peaks are superimposed upon a broad low intensity feature centered around 3311 cm^{-1}. There is good correlation between the infrared and Raman spectra. The observation of two OH stretching vibrations gives credence to the non-equivalence of the OH units in the herderite–hydroxylherderite structure. Such information is not available using other techniques such as X-ray diffraction.

Studies have shown a strong correlation between OH stretching frequencies and both O···O bond distances and H···O hydrogen bond distances [39–42]. Libowitzky showed that a regression function can be employed relating the hydroxyl stretching wavenumbers with regression coefficients better than 0.96 using infrared spectroscopy [43]. The function is described as: $\nu_1 = (3592 - 304) \times 109^{\frac{-d(O-O)}{0.1321}}$ cm^{-1}. Thus OH···O hydrogen bond distances may be calculated using the Libowitzky empirical function. Hydrogen bond distances may be obtained by using the OH stretching wavenumbers as given in Fig. 1. The values for the OH stretching vibrations listed above provide hydrogen bond distances of 2.9497 Å (3531 cm^{-1}), 3.0785 Å (3569 cm^{-1}), 3.1070 Å (3597 cm^{-1}), 3.1560 Å (3605 cm^{-1}). By using the position of the Raman OH stretching wavenumbers as given in Fig. 2, hydrogen bond distances may be estimated. Here, hydrogen bond distances are calculated as 3.0231 Å (3557 cm^{-1}), 3.0729 Å (3568 cm^{-1}), 3.1441 Å (3578 cm^{-1}), 3.1561 Å (3609 cm^{-1}), 3.2530 Å (3626 cm^{-1}). It is observed that the hydrogen bond distances calculated from the infrared spectra are in a similar range as calculated from the Raman spectrum.

The large hydrogen bond distances which are present in hydroxylherderite can also be seen in other mixed anion minerals such as peisleyite and perhamite [44,45] where the distances ranging between 3.052(5) and 2.683(6) Å. Such hydrogen bond distances are typical of secondary minerals. A range of hydrogen bond distances are observed from reasonably strong to weak hydrogen bonding. This range of hydrogen bonding contributes to the stability of the mineral. Two types of OH units can be identified in the structure of hydroxylherderite. Structural data (X-ray diffraction) do not give us such information (Lager and Gibbs [18], Harlow and Hawthorn [19]). Importantly, for all of the members of the herderite–hydroxylherderite series, two OH stretching vibrations are observed. This shows that there are two non-equivalent OH units in the mineral structure. The duplication of the hydroxyl stretching vibrations is also observed in the NIR spectra (see below).

The hydrogen bond distances previously established can be used to predict the hydroxyl stretching wavenumbers. The spectrum of hydroxylherderite may be divided into two groups of OH stretching wavenumbers; namely 3500–3600 cm^{-1} and 3600–3650 cm^{-1}. This distinction suggests that the strength of the hydrogen bonds as measured by the hydrogen bond distances can also be divided into two groups according to the H-bond distances. An arbitrary cut-off point may be 3.40 Å based upon the wavenumber 3590 cm^{-1}. Thus the first bands listed above may be described as weak hydrogen bonds and the last two bands as

relatively strong hydrogen bonds. It should be noted that the infrared band at 1635 cm^{-1} is assigned to the water HOH bending mode (figure not shown). For normal hydrogen-bonded water this band occurs at around 1620 cm^{-1}. Thus the position of this band also indicates relatively weak hydrogen bonding in the mineral hydroxylherderite.

Near Infrared spectroscopy (NIR)

The near infrared spectra of (a) herderite, (b) hydroxylherderite-SAA073, intensity has been multiplied a factor of 2, (c) hydroxylherderite-SAA074, intensity has been multiplied a factor of 4, (d) hydroxylherderite-SAA075, intensity has been multiplied a factor of 2, and (e) hydroxylherderite-SAA076, intensity has been multiplied a factor of 5 are shown in Fig. 3. This figure shows obvious differences in the spectra of the five minerals of the herderite–hydroxylherderite series. Near-infrared spectroscopy is often referred to as proton spectroscopy. The reason is that the near infrared spectrum, in the main, contains the combination and overtones bands of the hydroxyl bands of the mid-infrared spectral range. Thus, any units which contain protons such as hydroxyl, amine, and CH will show bands in the NIR spectral region.

The spectra may be conveniently divided into sections. The NIR spectral region between 4000 and 6000 cm^{-1} region is the region where combination bands of the OH vibrations in the mid-infrared spectral region. The region between 6000 and 8000 cm^{-1} displays the bands which are the combination and overtone bands of the hydroxyl stretching bands from the mid-IR. The spectra in this spectral range are illustrated in Fig. 4. The spectral region between 10,000 and 12,000 cm^{-1} display bands which are due to the second overtone of OH stretching vibration of the mid-infrared spectrum. The spectra are reported in Fig. 5.

The NIR spectrum of herderite shows two bands at 6977 and 7058 cm^{-1}. The infrared spectrum of herderite displays two bands at 3567 and 3575 cm^{-1} assigned to the OH stretching vibrations. The bands at 6977 and 7058 $cm^{-1}$are attributed to the first overtone of the OH stretching fundamental. These bands are assigned to $2\nu_{OH}$. An additional band of lower intensity is observed at

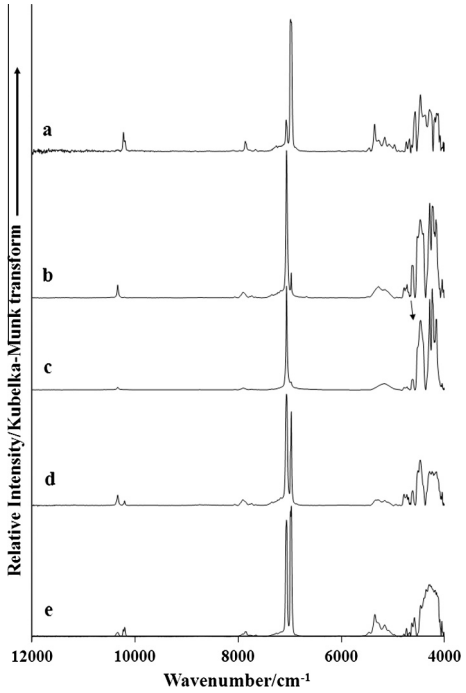

Fig. 3. Near-infrared spectrum of herderite–hydroxylherderite in the 4000–12,000 cm^{-1} region (samples SAA-073, 074, 075, 076 and 093).

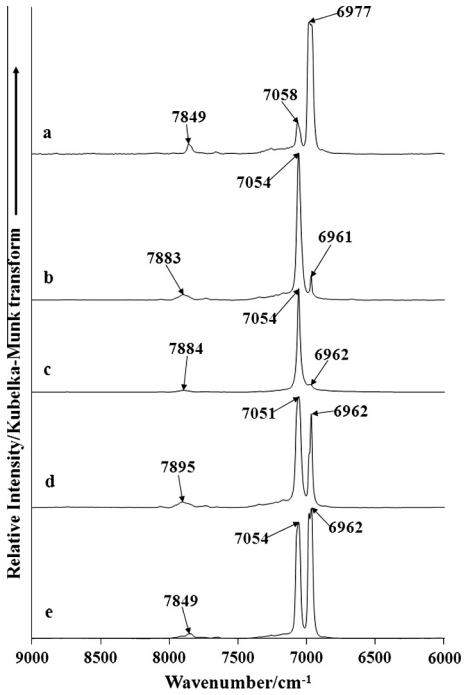

Fig. 4. Near-infrared spectrum of herderite–hydroxylherderite in the 6000–9000 cm^{-1} region (samples SAA-073, 074, 075, 076 and 093).

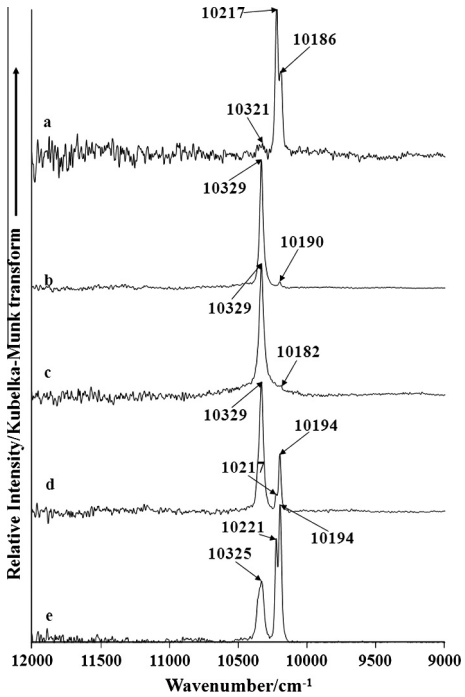

Fig. 5. Near-infrared spectrum of herderite–hydroxylherderite in the 90,000–12,000 cm^{-1} region (samples SAA-073, 074, 075, 076 and 093).

7849 cm^{-1}. This band is due to the combination of the stretching and deformation modes in the mid-infrared spectrum ($2\nu_{OH} + \delta_{OH}$) i.e. the band is due to the first overtone of the OH stretching fundamental and the OH deformation mode.

The NIR spectrum of hydroxylherderite (spectra b to e) displays two bands at around 6961 and 7054 cm^{-1}. The position of the bands remains constant but the intensity of the bands varies and appears to be a function of the fluorine content in the mineral as

Table 2
Variations of infrared, Raman and NIR OH bands and measured fluorine and calculated H_2O contents in wt.%.

	SAA-073	SAA-074	SAA-075	SAA-076	SAA-093	20,517[a]
wt.% (F)	0.24	0.07	1.90	4.46	8.01	5.71
N° atoms (F)	0.02	0.01	0.17	0.39	0.71	0.483
wt.% (H_2O)	5.28	5.42	4.53	3.37	1.58	2.90
N° atoms (OH)	0.98	0.99	0.83	0.61	0.29	0.517
F/(OH + F)	0.02	0.01	0.17	0.39	0.71	0.483
IR ν_{OH} (cm^{-1})	3605, 3597	3605, 3599	3605, 3600, 3566	3606	3575, 3567	–
IR δ_{OH} (cm^{-1})	776	773	776	776	788	–
Raman	3623	3623	3624, 3609	3626, 3609, 360	–	3625.8
NIR $2\nu_{OH}$	7054, 6961	7054, 6962	7051, 6962	7054, 6962	7058, 6977	–
NIR $3\nu_{OH}$	10,329, 10,190	10,329, 10,182	10,329,10,194	10,325, 10,194	10,321, 10,186	–

[a] According to Harlow and Hawthorne [19] and Harlow (personal communication).

reported in Table 2. The higher the fluorine content the greater the intensity of the 6962 cm^{-1} band. A low intensity NIR band is observed at around 7883 cm^{-1}. The position of this band appears to vary with the fluorine content. The position of the band (7849 cm^{-1}) is the same for the high fluorine content hydroxylherderite and herderite.

This spectral region is where the second overtone of the hydroxyl stretching fundamental that is $3\nu_{OH}$. The mineral herderite displays two bands at 10,186 and 10,217 cm^{-1} with a very weak band at 10,321 cm^{-1} (spectrum a). The two hydroxylherderite minerals with very low F content shows an intense band at 10,329 cm^{-1} with a very low intensity band at 10,190 cm^{-1}. For the two higher F content hydroxylherderite minerals two intense bands are observed at 10,194 and 10,329 cm^{-1}. The hydroxylherderite (spectrum e) has an additional band at 10,221 cm^{-1}. This band is also observed as a shoulder band in spectrum (d). It should be kept in mind that there are no quantum mechanical restrictions on the allowed vibrations on NIR spectroscopy. The combination of infrared and Raman bands is allowed. What is quite clear is that NIR spectroscopy shows differences in the spectra of the minerals and this is related to the F content of the minerals.

Conclusions

The samples associated to montebrasite and lepidolite rich pegmatites show lower fluorine values (SAA-073 – 0.24%; SAA-074 – 0.07%; SAA-075 – 1.90%) and the sample associated to triphylite rich pegmatite shows intermediate fluorine content (SAA-076 – 4.46%), while the analyzed sample from a muscovite and topaz rich pegmatite shows high fluorine (SAA-093 – 8.01%). This relationship may be explained in relation with the degree of differentiation of the pegmatite magma, where lithium rich pegmatites shows lower content of fluorine with predominance of hydroxylherderite in the hydrothermal system and the muscovite topaz rich pegmatite shows higher fluorine content with predominance of the F rich member herderite.

In the vibrational spectroscopic study, the Raman spectra of hydroxylherderite are characterized by bands at around 985 and 998 cm^{-1}, assigned to ν_1 symmetric stretching mode of the PO_4^{3-} units. Raman bands at around 1085, 1128 and 1138 cm^{-1} are attributed to both the HOP and PO antisymmetric stretching vibrations. The set of Raman bands observed at 563, 568, 577, 598, 616 and 633 cm^{-1} are assigned to the ν_4 out of plane bending modes of the PO_4 units. The OH Raman stretching vibrations of hydroxylherderite were observed ranging from 3626 cm^{-1} to 3609 cm^{-1}. The infrared stretching vibrations of hydroxylherderites were observed between 3606 cm^{-1} and 3599 cm^{-1}. The significance of two stretching vibrations in the OH stretching region, proves that there are two non-equivalent OH units in the structure of the herderite–hydroxylherderite series.

By using a Libowitzky type function, hydrogen bond distances based upon the infrared and Raman OH stretching band wavenumbers were calculated. By using the infrared OH stretching vibrations for sample SAA-073 the calculated hydrogen bond distances are: 2.9497 Å (3531 cm^{-1}), 3.0785 Å (3569 cm^{-1}), 3.1070 Å (3597 cm^{-1}), 3.1560 Å (3605 cm^{-1}). In agreement with the infrared data, the Raman OH stretching vibrations for sample SAA-076 shows similar values of calculated hydrogen bond distances, given as 3.0231 Å (3557 cm^{-1}), 3.0729 Å (3568 cm^{-1}), 3.1441 Å (3578 cm^{-1}), 3.1561 Å (3609 cm^{-1}), 3.2530 Å (3626 cm^{-1}).

Near infrared spectroscopy was used to characterize the herderite–hydroxylherderite minerals. Characteristic NIR bands at around 6961 and 7054 cm^{-1} were assigned to the first overtone of the fundamental, whilst NIR bands at 10,194 and 10,329 cm^{-1} are assigned to the second overtone of the fundamental OH stretching vibration.

The position and intensity of the infrared and near-infrared OH stretching bands show variations with fluorine content of the herderite–hydroxylherderite mineral series, in a similar correlation to that published data for amblygonite–montebrasite series [21,22]. The IR ν_{OH} bands for samples SAA-073 ($He_{0.01}Hy_{0.99}$) and SAA-093 ($He_{0.71}Hy_{0.29}$) are 3605, 3597 cm^{-1} and 3575, 3567 cm^{-1} respectively, and shows an increase of the position with increase of F content. The same correlation can be observed in the same samples in NIR $3\nu_{OH}$ bands. IR δ_{OH} bands where assigned at 776 cm^{-1} and 788 cm^{-1} and NIR $2\nu_{OH}$ bands where observed at 7054, 6961 cm^{-1} and 7058, 6977 cm^{-1} respectively, and shows an inverse correlation with decrease of position with increase of F content.

Acknowledgements

The financial and infra-structure support of the Discipline of Nanotechnology and Molecular Science, Science and Engineering Faculty of the Queensland University of Technology, is gratefully acknowledged. The Australian Research Council (ARC) is thanked for funding the instrumentation. R. Scholz thanks to CNPq – Conselho Nacional de Desenvolvimento Científico e Tecnológico (Grant No. 306287/2012-9). M. Cândido Filho thanks to CNPq/PIBIC/UFOP.

References

[1] H.G. Dill, Earth Sci. Rev. 100 (2010) 1–420.
[2] D.M. Burt, Met. Assoc. Acid Magmat. 1 (1974) 262–266.
[3] K. Rickers, R. Thomas, W.W. Heinrich, Min. Dep. 41 (2006) 229–245.
[4] R. Thomas, J.D. Webster, P. Davidson, Cont. Min. Pet. 161 (2011) 483–495.
[5] P.B. Moore, Min. Rec. 4 (1973) 103–130.
[6] D.M. Burt, Econ. Geol. 70 (1975) 1279–1292.
[7] P. Černý, Rev. Min. Geochem. 50 (2002) 405–444.
[8] I. Černá, P. Černý, J.B. Selway, R. Chapman, Can. Min. 40 (2002) 1339–1345.
[9] D. Atencio, J.M.V. Coutinho, L.A.D. Menezes, Axis 1 (2005) 1–18.
[10] D. Atencio, P.A. Matioli, J.B. Smith, N.V. Chukanov, J.M.V. Coutinho, R.K. Rastsvetaeva, S. Möckel, Amer. Min. 93 (2008) 1–6.

[11] P.J. Dunn, W. Wight, J. Gem. 15 (1976) 27–28.
[12] P.J. Dunn, C.W. Wolfe, P.B. Leavens, W.E. Wilson, Min. Rec. 10 (1979) 5–11.
[13] R.C. Kammerling, K. Scarratt, G. Bosshart, E.A. Jobbins, R.E. Kane, E.J. Gübelin, A.A. Levinson, J. Gem. 24 (1994) 3–40.
[14] W. Haidinger, Phil. Mag. Annals Phil. (London) New Series 4 (1828) 1–3.
[15] S.L. Penfield, Amer. J. Sci. 147 (1894) 329–339.
[16] C. Palache, H. Berman, C. Frondel, Dana's System of Mineralogy, seventh ed., Wiley, New York, 1951.
[17] K. Byrappa, D.Y. Pushcharovsky, Prog. Cryst. Growth Char. Mat. 24 (1992) 269–359.
[18] G.A. Lager, G.V. Gibbs, Amer. Min. 59 (1974) 919–925.
[19] G.E. Harlow, F.C. Hawthorne, Amer. Min. 93 (2008) 1545–1549.
[20] P.B. Leavens, P.J. Dunn, R.V. Gaines, Amer. Min. 63 (1978) 913–917.
[21] A.M. Fransolet, P. Tarte, Amer. Min. 62 (1977) 559–564.
[22] B. Rondeau, E. Fritsch, P. Lefevre, M. Guiraud, A.-M. Fransolet, Y. Lulzac, Can. Min. 44 (2006) 1109–1117.
[23] V.C. Farmer, Mineralogical Society Monograph 4: The Infrared Spectra of Minerals, London, 1974.
[24] R.L. Frost, K.L. Erickson, Spectrochim. Acta 61A (2004) 45–50.
[25] R.L. Frost, W. Martens, P.A. Williams, J.T. Kloprogge, Min. Mag. 66 (2002) 1063–1073.
[26] R.L. Frost, W. Martens, P.A. Williams, J.T. Kloprogge, J. Raman Spectrosc. 34 (2003) 751–759.
[27] R.L. Frost, W.N. Martens, T. Kloprogge, P.A. Williams, Neues Jahrb. Min. (2002) 481–496.
[28] R.L. Frost, M.L. Weier, J. Mol. Struct. 697 (2004) 207–211.
[29] K. Rickers, R. Thomas, W. Heinrich, Min. Dep. 41 (2006) 229–245.
[30] M.L. Frezzoti, F. Tecce, A. Casagli, J. Geochem. Explor. 112 (2012) 1–20.
[31] U. Kolitsch, D. Atencio, N.V. Chukanov, N.V. Zubkova, L.A.D.M. Filho, J.M.V. Coutinho, W.D. Birch, J. Schlüter, D. Pohl, A.R. Kampf, I.M. Steele, G. Favreau, L. Nasdala, S. Möckel, G. Giester, D.Y. Pushcharovsky, Min. Mag. 74 (2010) 469–486.
[32] R.L. Frost, P.A. Williams, W. Martens, J.T. Kloprogge, P. Leverett, J. Raman Spectrosc. 33 (2002) 260–263.
[33] C.E. Bamberger, W.R. Busing, G.M. Begun, R.G. Haire, L.C. Ellingboe, J. Solid State Chem. 57 (1985) 248–259.
[34] B.K. Choi, M.N. Lee, J.J. Kim, J. Raman Spectrosc. 20 (1989) 11–15.
[35] A. Galy, J. Phys. Radium 12 (1951) 827.
[36] H. Poulet, N. Toupry-Krauzman, Proc. Int. Conf. Raman, Spectrosc., 6th, vol. 2, 1978, pp. 364–365.
[37] N. Toupry-Krauzman, H. Poulet, M. Le Postollec, J. Raman Spectrosc. 8 (1979) 115–121.
[38] F.S. Casciani, R.A. Condrate, Sr., Proc. – Inter. Cong. Phosphorus Compounds, 2nd, 1980, pp. 175–190.
[39] J. Emsley, Chem. Soc. Rev. 9 (1980) 91–124.
[40] H. Lutz, Struct. Bond. 82 (1995) 85–103.
[41] W. Mikenda, J. Mol. Struct. 147 (1986) 1–15.
[42] A. Novak, Struct. Bond. 18 (1974) 177–216.
[43] E. Libowitsky, Monatsch. Chem. 130 (1999) 1047–1049.
[44] R.L. Frost, S.J. Mills, M.L. Weier, Peisleyite an unusual mixed anion mineral-a vibrational spectroscopic study, Spectrochim. Acta, Part A: Mol. Biomol. Spectrosc. 61A (2004) 177–184.
[45] R.L. Frost, M.L. Weier, S.J. Mills, Spectrochim. Acta 67A (2007) 604–610.